Induction of ID2 expression by hypoxia-inducible factor-1: ARole in dedifferentiation of hypoxic neuroblastoma cells.

Löfstedt, Tobias; Jögi, Annika; Sigvardsson, Mikael; Gradin, Katarina; Poellinger, Lorenz; Påhlman, Sven; Axelson, Håkan

Published in:
Journal of Biological Chemistry

DOI:
10.1074/jbc.M402904200

2004

JBC Papers in Press. Published on July 13, 2004 as Manuscript M402904200

Induction of *ID2* Expression by Hypoxia-Inducible Factor-1: A Role in Dedifferentiation of Hypoxic Neuroblastoma Cells.

Tobias Löfstedt[1], Annika Jögi[1], Mikael Sigvardsson[2], Katarina Gradin[3], Lorenz Poellinger[3], Sven Påhlman[1] and Håkan Axelson[1]

From the [1]Department of Laboratory Medicine, Division of Molecular Medicine, Lund University, University Hospital MAS, S-205 02 Malmö, Sweden; [2]Department of Medicine, Hematopoietic Stem Cell Laboratory, Lund University, BMC S-221 84 Lund, Sweden; and the [3]Department of Cell and Molecular Biology, Medical Nobel Institute, Karolinska Institute, S-171 77 Stockholm, Sweden.

Running title: Upregulation of *ID2* expression by HIF-1

Keywords: ID, hypoxia, HIF, neuroblastoma, dedifferentiation

Correspondence to: Håkan Axelson, Department of Laboratory Medicine, Division of Molecular Medicine, Lund University, University Hospital MAS, Entrance 78, S-205 02 Malmö, Sweden. Phone: +46-40337621; Fax: +46-40337322; E-mail: hakan.axelson@molmed.mas.lu.se

Abstract

ID (inhibitor of differentiation/ DNA binding) proteins, frequently deregulated in advanced human malignancies, can participate in multiple fundamental traits of cancer, such as block of differentiation, increased proliferation, tissue invasiveness and angiogenesis. We have previously demonstrated that hypoxia decreases expression of neuronal marker genes in neuroblastoma, but induces genes expressed in the neural crest, such as *ID2*. Due to its involvement in normal neural crest development and its ability to inhibit proneuronal bHLH proteins, the hypoxic induction of *ID2* was of particular interest. Here we report fast induction kinetics of *ID2* expression in hypoxic neuroblastoma cells. The upregulation of *ID2* was abolished by addition of actinomycin D, implicating a hypoxia-driven transcriptional mechanism. Analyzing the *ID2* promoter revealed several potential binding sites for hypoxia-inducible factors. Subsequent electrophoretic mobility shift and chromatin immunoprecipitation assays demonstrated two functional HIF-1 binding sites within *ID2* gene regulatory sequences located at –725 and –1893 relative to the transcriptional initiation point. In transfection assays, DNA-constructs of the *ID2* promoter, including the functional HIF-1 binding sites, induced luciferase reporter activity in a HIF-1 specific manner. These observations demonstrate that *ID2* is actively engaged by hypoxia and represents a novel HIF-1 target. Hypoxia-induced *ID2* expression could play a significant role in the previously observed dedifferentiation of hypoxic neuroblastoma cells, which in a clinical setting could lead to less mature and more aggressive tumors.

Introduction

In solid tumors the supply of oxygen and nutrients to some areas is often deprived due to a high rate of cellular proliferation that outpaces the rate of angiogenesis, and structurally abnormal vascularization leading to inadequate intratumoral blood circulation (1). In the resulting hypoxic microenvironment, cancer cells undergo adaptive changes that allow them to survive and even proliferate under hypoxic conditions (2). Mammalian cells, including cancer cells, adapt to hypoxia primarily through a transcriptional response pathway mediated by the hypoxia-inducible factors HIF-1 and HIF-2, which consist of an α subunit (HIF-1α or HIF-2α) and the constitutively expressed transcription factor ARNT/HIF-1β (3). At normoxia the α subunit is hydroxylated at critical proline residues by Fe(II)- and O_2-dependent prolyl hydroxylases (4,5) and proteasomally degraded via interaction with the von Hippel-Lindau tumor suppressor protein, pVHL (6,7). In addition to regulation of stability, hydroxylation of an asparagine residue within the α subunit negatively interferes with the function of the transactivation region of HIF under normoxic conditions (8). Hypoxia abrogates both proline and asparagine hydroxylation (4,8), leading to stable and functional HIFs that can bind regulatory HIF-binding sites (HBSs) of target genes involved in maintaining homeostasis, for instance *erythropoietin (EPO)* and *vascular endothelial growth factor* (*VEGF*) (9,10).

Neither primary tumors nor metastases will grow beyond a size of a few mm^3 in the absence of vascularization (11), but there is, paradoxically, an inverse correlation between the degree of tumor oxygenation and patient survival (12). Furthermore, hypoxic tumors appear to be more prone to invade surrounding tissue and to metastasize than better oxygenated ones (12,13). Since also HIF-1α overexpression has been found in most cancers it seems that increased adaptation to hypoxia enhances aggressive tumor behavior and progression to a lethal phenotype (3).

Neuroblastoma (NB), the most common extracranial solid pediatric tumor, arises where sympathetic nervous system (SNS) tissue forms (14,15). Depending on the differentiation stage of the tumor cells at diagnosis, the clinical behavior can be predicted, with immature tumors being more aggressive and having a poor prognosis (16,17). Neuroblastoma derives from immature sympathetic neural precursors, often with remaining neural crest traits (14,15,18). We have previously found that hypoxic neuroblastoma tumors and cells exposed to hypoxia (1% O_2) downregulate SNS marker genes, including the neuronal transcription factors *HASH-1* and *dHAND* (19), as well as the gene coding for the E-protein E2-2 (20). Concomitantly, hypoxia induces expression of genes involved in early neural crest development, in particular *NOTCH-1* and *ID2*, overall suggesting a dedifferentiation of neuroblastoma cells toward an immature neural crest-like phenotype (19). Moreover, hypoxic regions of mammary ductal carcinoma *in situ* (DCIS) and hypoxia-treated breast cancer cells have been shown to adopt a dedifferentiated phenotype, further implicating a roll of hypoxia on tumor maturation grade (21).

The ID (inhibitor of differentiation/DNA binding) proteins (ID1 - ID4) are part of the helix-loop-helix (HLH) family. They are direct or indirect negative regulators of basic helix-loop-helix (bHLH) transcription factors involved in cell lineage specification and in numerous developmental processes (22). Specifically, development of chicken neural crest from ectodermal precursors requires a proper regulation of *ID2* expression (23), an observation clearly relevant in the context of neuroblastoma, which originates from neural crest-derived precursors. Besides inhibiting/regulating differentiation, the ID proteins have been shown to bind important cell cycle regulatory proteins other than bHLH proteins, thereby promoting proliferation and also influencing cellular immortalization (24). Further, a large variety of human tumors display dysregulated expression of ID proteins (25-28). In

addition, an essential role of ID proteins in physiological and tumor angiogenesis as well as in tumor invasion has been demonstrated (25,29,30).

In the present study neuroblastoma cells demonstrated rapid induction of *ID2* when cultured at hypoxia (1% O_2). Hypoxia-induced upregulation of *ID2* was also seen in HeLa and human breast cancer MCF-7 and T47 cells, suggesting a general hypoxia-driven mechanism. These observations, together with a role of *ID2* in the specification of neuronal lineages derived from the neural crest, indicated a possible involvement of *ID2* in hypoxic neuroblastoma exhibiting neural crest-like features. Furthermore, the hypoxia-induced *ID2* expression was abrogated by actinomycin D treatment, indicating a requirement for HIF-directed RNA synthesis. When examining the 5´-flanking regulatory region of the *ID2* gene we found two sites that specifically bound HIF-1/ARNT heterodimers both *in vitro* and *in vivo*. These two functional HIF-binding sites induced luciferase reporter expression in HeLa cells when cotransfected with HIF-1 expression plasmids. Mutating the two HBSs decimated the HIF-1 specific upregulation. Overall, these results demonstrate that the *ID2* gene is transcriptionally upregulated in response to hypoxia via the HIF pathway. The activation of *ID2* could, in concert with downregulation of transcription factors involved in neuronal lineage specification, such as *dHAND*, *HASH-1* and *E2-2* (19,20), have a significant role in the dedifferentiation and progression of hypoxic neuroblastoma cells.

Experimental Procedures

Cell Culture. The following cell lines, maintained in conventional cell culture media, were used in this study: SK-N-BE(2), SH-SY5Y and IMR-32 neuroblastoma cells, HeLa cells, MCF-7 and T47 breast cancer cells, rat PC12 pheochromocytoma cells, and mouse NIH 3T3 fibroblasts. Under normoxic conditions, cells were incubated at 37 °C at an atmospheric pressure of 5% CO_2 and 95% air. Hypoxic conditions were created by flushing 5% CO_2 and

95% N_2 through a humidified chamber at 37 °C until an environment containing 1% O_2 was achieved, and measured with a MiniOX1 oxygen meter (Mine Safety Appliances Company). Induction of HIF-1 was also obtained by culturing cells at normoxic conditions with addition of 200 M 2,2´-dipyridyl (Sigma). In some experiments, to determine the transcriptional regulation of investigated genes, actinomycin D (Sigma) was added at a concentration of 5 g/ml medium.

Northern Blotting. Total RNA was prepared with Trizol reagent (Invitrogen), and 15 g of total RNA per lane was analyzed as previously described (19) with full-length human cDNA probes directed against *ID1*, *ID2* and *ID3* mRNA.

Real-Time Quantitative PCR. The relative gene expression levels of *ID1*, *ID2*, *ID3* and *VEGF* were determined by use of real-time quantitative PCR based on two-step SYBR green I chemistry (31,32). The Primer Express software (Applied Biosystems) was used for design of primer pairs (Table 1). Two g of total RNA, respectively extracted from SK-N-BE(2), SH-SY5Y and IMR-32 cells treated at hypoxia or normoxia, with or without 5 g/ml medium of actinomycin D (Sigma) for 0, 2, 4 and 8 h and purified with RNeasy kit (Quiagen), were used for cDNA synthesis with random hexamers and Superscript II RT-enzyme (Invitrogen). Obtained cDNA was diluted to 500 l in water and 5 l was used as template in each 25 l quantitative PCR. The amplification reactions were performed in a GeneAmp 5700 Sequence detector (Applied Biosystems), using a two-temperature cycling (10 min 95 °C and then 40 cycles of 95 °C for 15 s and 60 °C for 60 s). For detection of the PCR products in real-time the SYBR green I master mix (Eurogentec) was used. Four reference genes (*SDHA*, *YWHAZ*, *HMBS* and *UBC*), previously employed as expression references for neuroblastoma cell lines (31), and which were not regulated by growth under hypoxic conditions (data not shown)

were used for normalization of the expression data. Each reaction was performed in triplicates and the comparative Ct method was used for relative quantification of gene expression (32).

HIF-1 Binding-Site Search. A genomic region of 5000 bp upstream of the *ID2* transcriptional initiation site was determined using the NCBI Genomic BLAST program. This DNA sequence was then pasted into the DNA Strider 1.0 software, which was employed to locate putative HBSs. The search was based on compilations of functional HBSs and the HIF-1 binding consensus sequence BDCGTV (B = C/T/G, D = A/G/T, V = G/C/A), in turn established by previous definitions of consensus (33,34).

Western Blotting. Cells were lysed in RIPA buffer (10 mM Tris-HCl pH 7.2, 160 mM NaCl, 1% Triton X100, 1% sodium deoxycholate, 0.1% SDS, 1mM EDTA, 1mM EGTA) supplemented before use with Complete protease inhibitor cocktail (Roche). 80 μg of protein was separated by 6% SDS-PAGE and subsequently blotted onto Hybond C membranes (Amersham). The following primary antibodies were used: HIF-1α (mouse monoclonal, Novus Biologicals) and ARNT (rabbit polyclonal, Novus Biologicals). Super Signal substrate (Pierce) was used for chemiluminescence-based detection of appropriate secondary antibodies.

Nuclear Extract Preparation. A modified protocol from Fink *et al* (34) was used. Working on ice, cells were scraped into PBS and pelleted by centrifugation for 5 min at 2000 rpm at 4 °C. The pellet was resuspended in 4 packed cell volumes of cold hypotonic buffer (HB) containing 10 mM Tris-HCl pH 7.4, 10 mM KCl, 1.5 mM $MgCl_2$ and subsequently incubated 10 min on ice. Cells were then pelleted at 1500 rpm for 5 min at 4 °C and the pellet was resuspended in 4 packed cell volumes of lysis buffer (HB + 0.4% Nonidet NP-40). This

material was incubated for 10 min, whereafter the nuclei were pelleted by centrifugation at 1500 for 5 min at 4 °C. The pellet was then incubated in 2 packed cell volumes of high-salt buffer (HSB), containing 20 mM Tris-HCl pH 7.4, 0.42 M KCl, 1.5 mM $MgCl_2$, 0.2 M EDTA, 25% glycerol, for 20 min on ice with gentle agitation. Before use, both HB and HSB were supplemented with 20 μg/ml leupeptin and 1 μg/ml pepstatin (Roche) and HB was additionally complemented with 1 mM phenylmethylsulfonyl fluoride (PMSF) and 1 mM DTT. The nuclear debris was pelleted by centrifugation at 14000 rpm for 20 min at 4 °C. Obtained supernatant was aliquoted, frozen in liquid N_2 and stored at –80 °C.

Electrophoretic Mobility Shift Assay (EMSA). Table 2 summarizes sense oligonucleotide probes encompassing putative HIF-1 binding sites and corresponding mutant probes used in EMSAs. Synthesized probes (from Invitrogen) were end-labeled with [α-^{32}P]dATP (Amersham) by T4 polynucleotide kinase (Appligene), annealed and purified on G25 Microspin columns according to the manufacturer's instructions (Amersham). DNA-protein binding reactions were carried out in a buffer containing 20 mM Hepes pH 7.3, 50 mM KCl, 3 mM $MgCl_2$, 1 mM EDTA, 8% glycerol and 5 mM DTT for 20-30 min at 4 °C. Salmon sperm DNA at 1-20 ng/μl was added as bulk carrier DNA before binding reactions. Proteins were added in form of either 5 μg nuclear extract or *in vitro* synthesized HIF-1α and ARNT. The synthetic HIF-1 complex proteins were generated by coupled *in vitro* transcription/translation from pSP72/hHIF-1α and pGEM7/ARNT plasmids using rabbit reticulocyte lysate according to the manufacturer's guidelines (Promega). Before addition of buffer, equal aliquots (3 μl/binding reaction) of HIF-1α and ARNT proteins were allowed to associate for 30 min at room temperature. Annealed [α-^{32}P]dATP-labeled probes were used in all reactions at a specific activity of 25000 cpm. For competition experiments a 10- to 500-fold molar excess of unlabeled annealed probes was added to the binding reaction mixtures prior to addition of

labeled probes. For supershift analysis 1 µl of antibody directed against HIF-1α (mouse monoclonal, Novus Biologicals), ARNT (rabbit polyclonal, Novus Biologicals) or MYCN (mouse purified, PharMingen) was added to completed reaction mixtures and incubated for 1 h at 4 °C prior to electrophoresis. Samples were run on 4% non-denaturating polyacrylamid gels at 4 °C for 3-4 h. Electrophoresis was performed at 200 V, 12 mA in TBE buffer (89 mM Tris, 89 mM boric acid, 2 mM EDTA). Gels were then dried and autoradiographed.

Chromatin Immunoprecipitation (ChIP) Assay. SK-N-BE(2) cells were cultured with 200 µM DIP or control (normoxia, 21% O_2) for 4 h, washed once in PBS and then incubated in PBS + 1% formaldehyde at room temperature for 10 min. Cells were washed with ice-cold PBS and then scraped into cold 100 mM Tris-HCl (pH 8.7), 10 mM DTT, incubated for 15 min at 30 °C and subsequently pelleted at 4000 rpm for 5 min. Pellets were sequentially washed with cold PBS, Buffer I (0.25% Triton-X100, 10 mM EDTA, 0.5 mM EGTA, 10 mM HEPES pH = 6.5), and Buffer II (200 mM NaCl,1 mM EDTA, 0.5 mM EGTA, 10 mM HEPES pH = 6.5). Pellets were then resuspended in lysis buffer (1% SDS, 10 mM EDTA, 50 mM Tris-HCl pH = 8.0) containing 1x Complete protease inhibitor cocktail (Roche) and thereafter sonicated until DNA was approximately 500-700 bp in size. The samples were diluted 1:10 in 1% Triton-X100, 2 mM EDTA, 150 mM NaCl, 20 mM Tris-HCl pH = 8.0, 1x Complete protease inhibitor cocktail, and then incubated by rotation with 2 µg sheared salmon sperm DNA, 6 µg anti human IgG antibodies (rabbit polyclonal, abcam) and 45 µl 50% protein G-sepharose slurry (Amersham) for 2 h at 4 °C. Supernatant was collected by centrifugation at 3000 rpm for 15 s and incubated at 4 °C over night by rotation with antibodies against HIF-1α (mouse monoclonal, Novus Biologicals), or human IgG (rabbit polyclonal, abcam) as a negative control. Two µg of sheared salmon sperm DNA and 45 µl 50% protein G-sepharose slurry were then added and incubated by rotation for another 2 h at

4 °C. The Sepharose beads were collected at 3000 rpm for 15 s and sequentially washed for 15 min each under rotation with TSE I (0.1% SDS, Triton X-100, 2 mM EDTA, 20 mM Tris-HCl pH = 8.1, 150 mM NaCl), TSE II (0.1% SDS, Triton X-100, 2 mM EDTA, 20 mM Tris-HCl pH = 8.1, 500 mM NaCl) and Buffer III (0.25 M LiCl, 1% NP-40, 1% deoxycholate, 1 mM EDTA, 10 mM Tris-HCl pH = 8.1) at room temperature. Beads were washed three times with TE buffer followed by elution in 1% SDS, 0.1 M $NaHCO_3$ (3000 rpm, 15 s.). Supernatants were incubated over night at 65 °C and DNA was purified employing the PCR Purification Kit (Quiagen). The DNA was then used for 35 cycles of PCR together with primers flanking the putative HBSs within the *ID2* promoter: -1893-HBS f-GCTGCAATGTCCAAGAATCA, r-GAGTCCTCCCACAGTTCGAG, -725-HBS f-GTTGCAAAAGCCCACACTAAGC, r-GTTCACTGCAACCCATCGG. Primers flanking the HBS of the *VEGF* promoter were used as a positive control: f-GCCTCTGTCTGCCCAGCTGC, r-GTGGAGCTGAGAACGGGAAGC.

DNA Constructs and Site-Directed Mutagenesis. Plasmids containing genomic DNA fragments of the human *ID2* gene 5´-flanking region, respectively spanning from +35 to -1329 or -2755 relative transcriptional initiation, and inserted upstream of a luciferase reporter gene in pGL3-Basic vector, were kindly provided by Dr. T. Tokino, Department of Molecular Biology, Cancer Research Institute, Sapporo, Japan. Mutations were introduced into the p*ID2*-plasmids using the oligonucleotide-directed mutagenesis system QuickChange II XL (Stratagene) according to the manufacturer's instructions. All constructs and mutants were verified by sequencing employing the Big Dye Terminator v3.1 Cycle Sequencing Kit (Applied Biosystems).

Transfection and Luciferase Assay. Triplicates of 5 x 10^4 HeLa cells in 24-well culture plates (Costar) were separately transfected overnight with 0.2 μg each of the *ID2* promoter pGL3-Basic derivatives or empty pGL3-Basic vector, or a positive control vector containing three hypoxia-response elements in tandem, designated pHRE. For cotransfections, 0.4 μg of a pFLAG-mHIF-1α-(P402A,P563A) vector, expressing constitutively active HIF-1α (generous gift from Dr. Teresa Pereira, Karolinska Institute, Stockholm, Sweden) or 0.4 μg of empty pFLAG vector only was introduced. All transient transfections also included 0.1 μg of a *Renilla* luciferase control reporter plasmid, pRL-TK (Promega), and were performed using Lipofectin Reagent and Opti-MEM I Reduced Serum Medium (Invitrogen). Cells were harvested 24 h after transfection followed by measurement of luciferase activity using a Dual-Luciferase Reporter Assay System according to the manufacturer's instructions (Promega). The luciferase activity was defined as the ratio of *Photinus pyralis* luciferase activity from pGL3-Basic derivatives or pHRE relative to *Renilla reniformis* luciferase activity from pRL-TK, which reflected the efficiency of transfection.

Results

Induction of *ID2* and *ID1* Expression by Hypoxia. As observed earlier (19), expression of *ID2* was increased in neuroblastoma cells after 4 h of hypoxia (1% O_2) when compared to normoxic controls, as assessed by Northern blot analysis using total cellular RNA (Fig. 1, second panel). *ID2* induction could also be detected in breast cancer cells as well as in HeLa cells, but not in investigated rodent cells. *ID1* was also shown to be oxygen-regulated, with increased mRNA levels found in the tested neuroblastoma cells and in T47 breast cancer cells after 4 h under hypoxic conditions (Fig. 1, top panel). No hypoxia-dependent induction of *ID1* expression was however detected in MCF-7 breast cancer cells or HeLa cells. On the other hand, it should be noted that basal levels of *ID1* mRNA were relatively high in these cell

types, at normoxia as well as hypoxia. The third *ID* member expressed in neuroblastoma, *ID3*, appeared not to be hypoxia-induced in either neuroblastoma, breast cancer or HeLa cells, possibly with the exception of SK-N-BE(2) cells where higher levels were found compared to normoxic counterparts (Fig.1).

To focus on neuroblastoma, we investigated alterations in mRNA expression over time of the three *ID* genes at hypoxia and normoxia in neuroblastoma cells, using real-time quantitative PCR (qPCR). In terms of transcriptional regulation by hypoxia, we saw a fast induction of *ID2* gene expression at hypoxia when compared to normoxia (< 2 h) in all three neuroblastoma cell lines (Fig. 2B). The *ID2* upregulation was maintained throughout the investigated time-period of hypoxia-treatment. Hypoxia-induced expression was also observed for the *ID1* gene in a similar pattern as *ID2*, with rapid increase in mRNA levels and fluctuating peak quantities in the three neuroblastoma cell lines assayed (Fig. 2A). Hypoxia-treatment of neuroblastoma cells over the tested time-course did not result in higher *ID3* levels (Fig. 2C). Furthermore, after 4 h of treatment the levels of the three *ID* genes, as determined by real-time qPCR, were well in line with the results obtained from the Northern blot analyses. Since the gene encoding VEGF is a well-characterized HIF-1 target (10) and has previously been shown to be activated in neuroblastoma by hypoxia (19), we examined *VEGF* gene expression as an internal positive control in the real-time qPCR assays. As expected, hypoxia rapidly induced *VEGF* mRNA levels in all cell lines tested (Fig. 2D).

Since neuroblastoma originates from neural crest-derived sympathetic precursor cells and *ID2* regulates neural crest specification, our focus was hereafter directed on the hypoxic regulation of *ID2*.

Hypoxia Induces *ID2* mRNA at a Transcriptional Level. In order to clarify whether hypoxia augmented *ID2* mRNA at the level of mRNA stability or transcription, SK-N-BE(2)

and SH-SY5Y cells were exposed to normoxia or hypoxia in the absence or presence of actinomycin D. Treatment with actinomycin D, which blocks the function of the transcriptional machinery, completely abolished the hypoxia-induced upregulation of *ID2* in both cell-lines tested (Fig. 3A), indicating that hypoxia regulates *ID2* by a transcriptional mechanism. As a positive control, the effect of actinomycin D on hypoxia- and HIF-induced *VEGF* upregulation was examined. When cells were treated with actinomycin D, the expression pattern of *VEGF* was almost the same between normoxic and hypoxic conditions (Fig. 3B), confirming that actinomycin D blocked HIF-induced target gene activation. These results suggest that *ID2* is induced by hypoxia via a rapidly acting transcriptional mechanism, implicating involvement of hypoxia-inducible factors.

Identification of Functional HIF-Binding Sites in the *ID2* Promoter. Since the hypoxic induction pattern of *ID2* appeared to be regulated through fast neosynthesis of mRNA, we wanted to investigate if *ID2* was a HIF target. When examining the *ID2* promoter for putative HIF-binding sites (HBSs), we found several sites sharing homology with the HIF-binding consensus sequence BDCGTV (B = C/T/G, D = A/G/T, V = G/C/A). Eight potential HBSs were selected for investigation based on their sequence similarities with the most common functional HBSs reported earlier (33), and their localization relative the transcriptional initiation site of the *ID2* gene (see Table 2). The selected sites were tested for binding of the HIF complex in electrophoretic mobility shift assays (EMSAs). HIF proteins were added to the EMSA gels as either nuclear extracts, or as *in vitro* generated HIF-1 and ARNT proteins that had been allowed to associate before complementation to EMSA binding reactions. Nuclear extracts were prepared from SK-N-BE(2) cells cultured for 4 h under normoxic or hypoxic (1% O_2) conditions, or treated with 200 M 2,2´-dipyridyl (DIP) for 4 h. DIP is a cell-permeable iron chelator that functions by inhibiting the Fe(II)- and O_2-dependent prolyl

hydroxylases (4), thereby strongly stabilizing HIF-1α proteins (Fig. 4A). Of the eight examined putative HIF-binding sites within the *ID2* gene promoter, two sites located at -1893 (CACGTA) and -725 (TGCGTG) in relation to start of transcription, displayed specific HIF-1 binding in our assays.

First, the -1893-HBS was demonstrated to bind HIF-1 complexes from nuclear extracts of DIP-treated SK-N-BE(2) cells (Fig. 4B). This binding could effectively be competed out using non-radiolabeled wildtype -1893-HBS oligonucleotide probes in excess (compare lane 3 with lanes 5 and 7, Fig 4B). Competition with non-radiolabeled mutant probes, where two nucleotides in the HIF-binding sequence had been exchanged (CACGTA → CA**AT**TA), did not diminish the DIP-induced signal to the same extent as wildtype probes did, demonstrating specific HIF-1 binding to the -1893-HBS (see lanes 9 and 11, Fig. 4B). The specificity was further verified by adding an antibody directed against HIF-1α to the EMSA binding reactions, which supershifted the DIP-induced band (Fig. 4B, lane 13). Confirmation of HIF-binding to the -1893-HBS was also performed in EMSAs where *in vitro* synthesized HIF-1α and ARNT proteins were included. A previously identified functional HBS from *erythropoietin* (*EPO*) gene regulatory regions (9) was utilized as a positive control. As expected, *in vitro* generated HIF-1 and also DIP-induced HIF-1 complexes from SK-N-BE(2) nuclear extracts bound this site (Fig. 5 and data not shown). This binding was further detected with the *ID2*-derived -1893-HBS (Fig. 5). Antibodies directed against HIF-1α or ARNT respectively supershifted or disrupted the HIF-1 complex binding to both the *EPO* HBS and the -1893 HBS in identical patterns (Fig. 5, lanes 3, 4 and 10, 11).

Functionality of the -725-HBS was demonstrated by specific binding of *in vitro* synthesized HIF-1 proteins (Fig. 6). Using an excess of non-radiolabeled wildtype -725-HBS probes resulted in effective competition of this binding, which was not obtained to the same degree with mutant (TGCGTG → TG**AA**TG) non-radiolabeled probes (Fig. 6, compare lanes

4 and 5 with 6 and 7, respectively). Supershift experiments using an anti-HIF-1α antibody verified that binding complexes contained HIF-1α. (Fig. 6, lanes 8 and 9). Negative control experiments, employing an antibody directed against MYCN did not result in shift of migration in any of our assays (data not shown). HIF-1α or ARNT proteins alone did not bind to any HBS tested by EMSA. Moreover, EMSAs conducted with the *ID2* -1893-HBS and nuclear extracts prepared from hypoxic SK-N-BE(2) cells induced a treatment-specific HIF-1 band, which could be reduced with an excess of non-labeled wt-1893-HBS probes as well as with wt-EPO-HBS probes (Fig. 7). This competition was not obtained by addition of non-radiolabeled mutated -1893-HBS probes or excess of oligonucleotides encompassing an *ID2*-derived putative HBS located at -93, determined as non-functional in our EMSA experiments (Fig. 7 and data not shown). Remaining potential *ID2* HBSs tested here did not exhibit any HIF-1 binding with neither nuclear extract nor *in vitro* generated HIF-1 complex proteins (data not shown).

HIF-1 Binds the *ID2* Promoter In Vivo. SK-N-BE(2) neuroblastoma cells were cultured for 4 h with 200 μM DIP in order to induce stable and functional HIF proteins, in parallel with untreated control cells. Cells were incubated with formaldehyde, lysed and sonicated until most DNA was 500-700 bp in size. Respective samples were subjected to chromatin immunoprecipitations after which DNA fragments could be collected, purified and used in PCR reactions together with primers flanking the *ID2* promoter sites, previously demonstrated in EMSAs to bind HIF-1 proteins. As shown in Figure 8A, HIF-1 bound both the -1893 site and the -725 site in DIP-treated SK-N-BE(2) cells to a much higher extent than control cells. Performing negative control immunoprecipitations of DIP-treated SK-N-BE(2) cell extracts, using anti human IgG antibodies, did not result in any substantial amplification of DNA fragments encompassing the *ID2* promoter HBSs (Fig. 8A). These results indicated specific

HIF-1 binding to the *ID2* promoter in neuroblastoma cells, under conditions where HIF proteins were stabilized. As an internal positive control, primers flanking the HIF-binding site of the *VEGF* promoter were used in PCR reactions together with immunoprecipitated DNA. SK-N-BE(2) cells treated with DIP demonstrated HIF-1 binding to the *VEGF* promoter at a much higher level compared with untreated cells (Fig. 8B). Moreover, DNA fragments containing the *VEGF* HBS were not amplified in PCR reactions after immunoprecipitations using anti IgG antibodies (Fig. 8B).

Transcriptional Activation of the *ID2* Promoter by HIF-1. After confirming specific binding of HIF-1 complexes to the two HBSs located within *ID2* gene regulatory sequences, we wanted to investigate their involvement in the hypoxia-activated *ID2* expression demonstrated earlier. Plasmids containing the *ID2* gene promoter, coupled upstream of a luciferase reporter gene, were used in transient cotransfections of HeLa cells together with plasmids expressing constitutively active HIF-1α cDNA, and internal Renilla luciferase-expressing plasmids controlling efficiency of transfection. When the p*ID2*-1329wt plasmids were employed, containing the -725 HIF-binding site, pFLAG-HIF-1α induced reporter gene expression to an approximate 8-fold when compared to the activity induced by pFLAG vector only (Fig. 9). *ID2* promoter constructs containing both of the functional HBSs, p*ID2*-2755wt plasmids, raised luciferase reporter activity to a 12-fold upon addition of HIF-1α compared to addition of empty vector alone. However, when introducing mutations into the -1893 and -725 HIF-binding sites, reporter gene-induction by HIF-1α was substantially reduced (Fig. 9). HIF-1α did not augment luciferase expression from empty pGL3-Basic vector. The positive control vector pHRE, containing three functional HIF-binding sites, generated more than a 21-fold reporter gene upregulation upon introduction of pFLAG-HIF-1α compared to empty pFLAG vector, demonstrating functionality of the assay (Fig. 9).

Discussion

In this report, we show that the *ID2* gene is transcriptionally activated in response to hypoxia through a mechanism that involves binding of HIF-1α/ARNT complexes to sites located within the promoter region. This conclusion is based on the following observations. First, *ID2* expression was upregulated by hypoxia (1% O_2) in three human neuroblastoma and two breast cancer cell lines and in HeLa cells. Second, the hypoxia-induced expression of *ID2* in neuroblastoma cells was as fast as the upregulation of *VEGF*, an established HIF-1 target gene (10,35). The level of *ID2* induction was, however, lower than the corresponding *VEGF* upregulation, probably reflecting the fact that ID2 is a transcription factor, the expression of which needs to be firmly regulated due to its involvement in several intracellular processes (36). Third, blocking the transcriptional machinery by treatment with actinomycin D completely disrupted the hypoxia-induced *ID2* expression in both cell-lines tested. Fourth, two sites respectively located at -725 (5´-TGCGTG-3´) and -1893 (5´-CACGTA-3´) within the *ID2* promoter demonstrated specific binding to HIF-1 complexes derived from *in vitro* synthesis, or from nuclear extracts of cells cultured at ambient or chemically induced hypoxia. This binding was well in magnitude with HIF-1 binding to an *erythropoietin*-derived HBS, which could also block HIF-1 binding to the -1893 HBS. Furthermore, performing chromatin immunoprecipitations on DIP-treated SK-N-BE(2) neuroblastoma cells displayed specific HIF-1 binding to the *ID2*-derived HBSs also in the *in vivo* situation. Finally, *ID2* promoter constructs, containing the HIF-1 binding sites in wildtype configuration, induced reporter gene expression in cells cotransfected with vectors expressing HIF-1α to a markedly higher extent than *ID2* promoter vectors carrying mutations in the functional HBSs. However, HIF-1-induced *ID2* promoter activity was still present when the two functional HBSs were mutated (Fig. 9) indicating requirements of additional transcription factors in the hypoxic setting. Lately, chimeric proteins of EWS and ETS transcription factors have been shown to

upregulate *ID2* expression in Ewing sarcoma by binding to characterized sites within the *ID2* promoter (37,38). Since *ETS-1* has been demonstrated to be a direct HIF-1 target gene and is upregulated by hypoxia (39), binding of ETS proteins to the *ID2* promoter could be a possible explanation for the hypoxia-induced reporter gene activation observed after mutating the functional HBSs. It is also possible, however unlikely, that previously unidentified non-consensus HIF-binding sites, potentially located in the investigated promoter regions, were responsible for the remaining hypoxia-induced reporter activity.

Hypoxic upregulation of *ID2* could have numerous important implications in the progression of neuroblastoma, and likely other tumors as well. The ID proteins are thought to affect the balance between cell growth and differentiation, generally promoting proliferation in a large variety of cell types (40-42). Several mechanisms have been reported for this growth promoting effect. By binding to and possibly inactivating Rb family proteins, ID proteins could relieve E2F transcription from the repressive influence of Rb and inhibit antiproliferative signaling, thereby allowing G1- to S-phase transition of the cell cycle (43). ID proteins have also been shown to affect the cell cycle by indirectly down-regulating the expression of cyclin-dependent kinase inhibitors $p21^{Cip1}$ and $p16^{INK4a}$, which could inhibit the Rb pathway in an alternative manner (44,45). Furthermore, since ID proteins, which are often deregulated in tumors also have been found to confer features of transformation and immortalization in addition to promoting proliferation, when overexpressed in cell culture and *in vivo*, these capabilities would all be advantageous for tumor progression. Even though hypoxia-treatment of cultured neuroblastoma cells over time appeared without an increase in cell growth compared to normoxic cells, xenografted hypoxic SK-N-BE(2) cells resulted in slightly larger and faster growing tumors than corresponding lesions from control cells (19). Hypoxia-induced *ID2* and *ID1* expression might therefore be involved in the control of tumor cell growth *in vivo*.

We have earlier demonstrated that expression of *ID* genes is downregulated upon induced differentiation of neuroblastoma cell lines (46), which is also the case in many other cell types (47-49). Conversely, ectopic expression of ID inhibits differentiation of most, if not all, cell types and tissues investigated so far (22). In agreement with these earlier findings we recently found in neuroblastoma that hypoxia down-regulates SNS marker genes, including the lineage-specifying transcription factors *HASH-1* and *dHAND*, while concomitantly inducing genes expressed in early neural crest development, among them *ID2* (19). Thus, the hypoxic cells adopt an immature phenotype where *ID2* could play a significant part, primarily by sequestering E-proteins, preventing their ability to bind DNA in heterodimeric complexes together with bHLH proteins such as HASH-1 and dHAND (46,47). Recently, evidence have emerged demonstrating how ID proteins effectively sequesters pools of transiently diffusing E-proteins and abolish bHLH chromatin association (50). Furthermore, we have also demonstrated that hypoxia downregulates gene expression of the dimerization partner for ID2, dHAND and HASH-1 (46), the bHLH E-protein E2-2 (20). Based on these findings we propose a model for dedifferentiation in hypoxic neuroblastoma cells as depicted in Fig. 10.

In the present study hypoxia-induced upregulation of *ID2* (and *ID1*) was also detected in breast cancer cells, previously shown to be dedifferentiated in response to hypoxia (21). Given the multitude of influences dysregulated ID proteins could have on tumor progression, it is likely that hypoxia-activated *ID2* and/or *ID1* are important factors also in the breast tumor situation. Generally, tumor aggressiveness and tumor cell differentiation are well correlated, which is exhibited in neuroblastoma where highly malignant tumors express low levels of neuronal differentiation markers (16). Clinically, neuroblastoma aggressiveness relies in the ability to metastasize and our group has previously suggested that the hypoxia-induced shift toward a neural crest-like phenotype, conferring higher migratory capacity,

would generate more aggressive tumor cells with increased potential to metastasize (19). In agreement with this suggestion are earlier investigations showing more frequent invasion and higher metastatic ability by poorly oxygenated tumors compared with better oxygenated ones (12,13).

Recent studies have shown that loss of *ID1* and *ID3* result in premature differentiation during neurogenesis but also severe defects in angiogenesis within the brain, both under normal development and in three different xenografted tumors (25). The *ID* loss was displayed by blood vessels lacking the ability to branch and sprout, and defective formation of normal caliber lumens during tumor progression. Since *ID2* is expressed outside the central nervous system (CNS), it is reasonable that the confinement of the *ID1*/*ID3* knockout defects to the CNS is a result of compensation outside the CNS, indirectly associating *ID2* with involvement in angiogenesis (51). Several mechanisms are now emerging by which ID proteins could contribute to angiogenesis, involving transcriptional repression of angiogenesis inhibitors (52) as well as regulation of proangiogenic proteins, all exhibiting decrease upon loss of ID (53). Physiological and tumor angiogenesis is largely dependent on proper VEGF signaling, which is induced by HIF-1 (and HIF-2) and, interestingly, which can be decreased by loss of *ID* function (25). Overall, ID proteins seem to be involved in several of the fundamental characteristics that constitute tumor and cancer cell behavior. Hypoxic induction of *ID2* in neuroblastoma and other tumor types could have important implications on these features, leading to strongly proliferative, less mature and more malignant tumors.

References

1. Carmeliet, P., and Jain, R. K. (2000) *Nature* **407**, 249-257.
2. Harris, A. L. (2002) *Nat. Rev. Cancer* **2**, 38-47
3. Semenza, G. L. (1999) *Annu. Rev. Cell Dev. Biol.* **15**, 551-578
4. Bruick, R. K., and McKnight, S.L. (2001) *Science* **294**, 1337-1340
5. Epstein, A. C., Gleadle, J.M., McNeill, L.A., Hewitson, K.S., O'Rourke, J., Mole, D.R., Mukherji, M., Metzen, E., Wilson, M.I., Dhanda, A., Tian, Y.M., Masson, N., Hamilton, D.L., Jaakkola, P., Barstead, R., Hodgkin, J., Maxwell, P.H., Pugh, C.W., Schofield, C.J., and Ratcliffe, P.J. (2001) *Cell* **107**, 1-3
6. Tanimoto, K., Makino, Y., Pereira, T., Poellinger, L. (2000) *EMBO J.* **19**, 4298-4309
7. Ohh, M., Park, C. W., Ivan, M., Hoffman, M. A., Kim, T. Y., Huang, L. E., Pavletich, N., Chau, V., and Kaelin, W. G. (2000) *Nat. Cell Biol.* **2**, 423-427
8. Lando, D., Peet, D. J., Whelan, D. A., Gorman, J. J., and Whitelaw, M. L. (2002) *Science* **295**, 858-861.
9. Wang, G. L., and Semenza, G. L. (1993) *J. Biol. Chem.* **268**, 21513-21518
10. Forsythe, J. A., Jiang, B. H., Iyer, N. V., Agani, F., Leung, S. W., Koos, R. D., and Semenza, G. L. (1996) *Mol. Cell Biol.* **16**, 4604-4613
11. Hanahan, D., and Folkman, J. (1996) *Cell* **86**, 353-364.
12. Hockel, M., Schlenger, K., Aral, B., Mitze, M., Schaffer, U., and Vaupel, P. (1996) *Cancer Res.* **56**, 4509-4515
13. Brizel, D. M., Scully, S. P., Harrelson, J. M., Layfield, L. J., Bean, J. M., Prosnitz, L. R., and Dewhirst, M. W. (1996) *Cancer Res.* **56**, 941-943
14. Hoehner, J. C., Gestblom, C., Hedborg, F., Sandstedt, B., Olsen, L., Påhlman, S. (1996) *Lab. Invest.* **75**, 659-675
15. Påhlman, S., Hedborg, F. (2000) Development of the Neural Crest and Sympathetic Nervous System. In: Brodeur, G. M., Sawada, T., Tsuchida, Y., Voute, P. A. (ed). *Neuroblastoma*, Elsevier Science, Amsterdam
16. Hedborg, F., Bjelfman, C., Sparen, P., Sandstedt, B., and Påhlman, S. (1995) *Eur. J. Cancer* **31A**, 435-443
17. Brodeur, G. M. (2003) *Nat. Rev. Cancer* **3**, 203-216
18. Gestblom, C., Grynfeld, A., Øra, I., Örtoft, E., Larsson, C., Axelson, H., Sandstedt, B., Cserjesi, P., Olson, E. N., and Påhlman, S. (1999) *Lab. Invest.* **79**, 67-79
19. Jögi, A., Øra, I., Nilsson, H., Lindeheim, A., Makino, Y., Poellinger, L., Axelson, H., and Påhlman, S. (2002) *Proc. Natl. Acad. Sci. U. S. A.* **99**, 7021-7026
20. Jögi, A., Vallon-Christersson, J., Holmquist, L., Axelson, H., Borg, Å., and Påhlman, S. (2004) *Exp. Cell. Res.* **295**, 469-487
21. Helczynska, K., Kronblad, Å., Jögi, A., Nilsson, E., Beckman, S., Landberg, G., and Påhlman, S. (2003) *Cancer Res.* **63**, 1441-1444
22. Yokota, Y. (2001) *Oncogene* **20**, 8290-8298
23. Martinsen, B. J., and Bronner-Fraser, M. (1998) *Science* **281**, 988-991
24. Zebedee, Z., and Hara, E. (2001) *Oncogene* **20**, 8317-8325
25. Lyden, D., Young, A. Z., Zagzag, D., Yan, W., Gerald, W., O'Reilly, R., Bader, B. L., Hynes, R. O., Zhuang, Y., Manova, K., and Benezra, R. (1999) *Nature* **401**, 670-677
26. Maruyama, H., Kleeff, J., Wildi, S., Friess, H., Buchler, M. W., Israel, M. A., and Korc, M. (1999) *Am. J. Pathol.* **155**, 815-822
27. Langlands, K., Down, G. A., and Kealey, T. (2000) *Cancer Res* **60**, 5929-5933
28. Lin, C. Q., Singh, J., Murata, K., Itahana, Y., Parrinello, S., Liang, S. H., Gillett, C. E., Campisi, J., and Desprez, P. Y. (2000) *Cancer Res.* **60**, 1332-1340

29. Desprez, P. Y., Hara, E., Bissell, M. J., and Campisi, J. (1995) *Mol. Cell Biol.* **15**, 3398-3404
30. Desprez, P. Y., Lin, C. Q., Thomasset, N., Sympson, C. J., Bissell, M. J., and Campisi, J. (1998) *Mol. Cell Biol.* **18**, 4577-4588
31. Vandesompele, J., De Paepe, A., and Speleman, F. (2002) *Anal. Biochem.* **303**, 95-98
32. De Preter, K., Speleman, F., Combaret, V., Lunec, J., Laureys, G., Eussen, B. H., Francotte, N., Board, J., Pearson, A. D., De Paepe, A., Van Roy, N., and Vandesompele, J. (2002) *Mod. Pathol.* **15**, 159-166
33. Camenisch, G., Stroka, D. M., Gassmann, M., and Wenger, R. H. (2001) *Pflügers Arch.* **443**, 240-249
34. Fink, T., Kazlauskas, A., Poellinger, L., Ebbesen, P., and Zachar, V. (2002) *Blood* **99**, 2077-2083.
35. Carmeliet, P., Dor, Y., Herbert, J. M., Fukumura, D., Brusselmans, K., Dewerchin, M., Neeman, M., Bono, F., Abramovitch, R., Maxwell, P., Koch, C. J., Ratcliffe, P., Moons, L., Jain, R. K., Collen, D., Keshert, E., and Keshet, E. (1998) *Nature* **394**, 485-490.
36. Yokota, Y., and Mori, S. (2002) *J. Cell Physiol.* **190**, 21-28
37. Nishimori, H., Sasaki, Y., Yoshida, K., Irifune, H., Zembutsu, H., Tanaka, T., Aoyama, T., Hosaka, T., Kawaguchi, S., Wada, T., Hata, J., Toguchida, J., Nakamura, Y., and Tokino, T. (2002) *Oncogene* **21**, 8302-8309
38. Fukuma, M., Okita, H., Hata, J., and Umezawa, A. (2003) *Oncogene* **22**, 1-9
39. Oikawa, M., Abe, M., Kurosawa, H., Hida, W., Shirato, K., and Sato, Y. (2001) *Biochem. Biophys. Res. Commun.* **289**, 39-43
40. Barone, M. V., Pepperkok, R., Peverali, F. A., and Philipson, L. (1994) *Proc. Natl. Acad. Sci. U. S. A.* **91**, 4985-4988
41. Mori, S., Nishikawa, S.I., and Yokota, Y. (2000) *EMBO J.* **19**, 5772-5781
42. Wang, S., Sdrulla, A., Johnson, J. E., Yokota, Y., and Barres, B. A. (2001) *Neuron* **29**, 603-614
43. Lasorella, A., Noseda, M., Beyna, M., Yokota, Y., and Iavarone, A. (2000) *Nature* **407**, 592-598.
44. Prabhu, S., Ignatova, A., Park, S. T., and Sun, X. H. (1997) *Mol. Cell Biol.* **17**, 5888-5896
45. Ohtani, N., Zebedee, Z., Huot, T. J., Stinson, J. A., Sugimoto, M., Ohashi, Y., Sharrocks, A. D., Peters, G., and Hara, E. (2001) *Nature* **409**, 1067-1070
46. Jögi, A., Persson, P., Grynfeld, A., Påhlman, S., and Axelson, H. (2002) *J. Biol. Chem.* **277**, 9118-9126
47. Benezra, R., Davis, R.L., Lockshon, D., Turner, D.L., and Weintraub, H. (1990) *Cell* **61**, 49-59
48. Sun, X. H., Copeland, N. G., Jenkins, N. A., and Baltimore, D. (1991) *Mol. Cell Biol.* **11**, 5603-5611
49. Einarson, M. B., and Chao, M. V. (1995) *Mol. Cell Biol.* **15**, 4175-4183
50. O'Toole, P. J., Inoue, T., Emerson, L., Morrison, I. E., Mackie, A. R., Cherry, R. J., and Norton, J. D. (2003) *J. Biol. Chem.* **278**, 45770-45776
51. Benezra, R., Rafii, S., and Lyden, D. (2001) *Oncogene* **20**, 8334-8341
52. Volpert, O. V., Pili, R., Sikder, H. A., Nelius, T., Zaichuk, T., Morris, C., Shiflett, C. B., Devlin, M. K., Conant, K., and Alani, R. M. (2002) *Cancer Cell* **2**, 473-483
53. Ruzinova, M. B., Schoer, R. A., Gerald, W., Egan, J. E., Pandolfi, P. P., Rafii, S., Manova, K., Mittal, V., and Benezra, R. (2003) *Cancer Cell* **4**, 277-289

Footnotes

[1]Supported by grants from the Swedish Cancer Society, the Children's Cancer Foundation of Sweden, Åke Wiberg's Foundation, HKH Kronprinsessan Lovisas förening för barnasjukvård, Hans von Kantzow's Foundation, Ollie and Elof Ericsson's foundation, the Crafoord Foundation and Malmö University Hospital Research Funds.

[2]The abbreviations used are: HIF, hypoxia-inducible factor; HBS, HIF-binding site; ID, inhibitor of DNA-binding/differentiation; ARNT, aryl hydrocarbon receptor nuclear translocator; HASH-1, human achaete-scute homolog-1; dHAND, deciduum heart autonomic nervous system and neural crest derivatives; HLH, helix-loop-helix; bHLH, basic helix-loop-helix

Figure Legends

FIG. 1. ***ID* expression in response to hypoxia and normoxia.** Neuroblastoma (IMR-32, SH-SY5Y, SK-N-BE(2)), breast cancer (MCF-7, T47), rat pheochromocytoma PC12 and mouse fibroblast NIH 3T3 cells were cultured at hypoxia, 1% O_2, (H) or normoxia, 21% O_2, (N) for 4 h and subsequently subjected to RNA preparation. Northern blot analysis was performed with total RNA (15 μg/lane) and indicated full-length cDNA probes. We used 28S-RNA as an internal loading control.

FIG. 2. **Rapid upregulation of *ID2* and *ID1* by hypoxia.** Real-time quantitative PCR experiments showing induction kinetics of *ID* genes and *VEGF* in neuroblastoma cells treated at hypoxia, 1% O_2, (H) or normoxia, 21% O_2, (N) for 0, 2, 4 and 8 h. Two μg of RNA was extracted per cell-line and used for cDNA synthesis, out of which 0.8 ng was included in every 25 μl qPCR reaction. Triplicates for each gene and every time-point were performed and the comparative Ct method was utilized for data analysis (32). Normalization of the *ID* and *VEGF* expression data was carried out using four reference genes (SDHA, YWHAZ, HMBS and UBC), which were not visibly influenced by hypoxia (data not shown). Values obtained at 0 h of treatment were set to 1.0. Results are representative of two independent experiments and indicated as mean ± S.E. (bars).

FIG. 3. **Hypoxia upregulates *ID2* via a transcriptional mechanism**. Real-time quantitative PCR experiments demonstrating the impact of actinomycin D-treatment on hypoxic induction of *ID2* and *VEGF*. SK-N-BE(2) and SH-SY5Y cells were cultured under hypoxic, 1% O_2, (H) or normoxic (N) conditions for 0, 2 and 4 hours, with or without actinomycin D (+ AD) at a concentration of 5 μg/ml medium. All qPCR reactions were carried out in triplicates and

normalized as described (see Experimental Procedures). Data are presented as mean ± S.E. (bars).

FIG. 4. **DIP stabilizes HIF-1α expression and induces HIF-1 binding to a site within the *ID2* promoter.** *A*, Western blot analysis of HIF-1α expression in SK-N-BE(2) cells treated for 4 h with 200 μM 2,2´-dipyridyl (D) or normoxic control cells (c). ARNT was used as a loading control. *B*, EMSA showing HIF-1 binding to the *ID2*-derived -1893 HIF-1 binding site. Five μg of nuclear extracts from DIP-treated (D) SK-N-BE(2) cells or control cells (c) were included in protein-DNA binding reactions. Competition experiments were conducted with either wildtype (wt) or mutant (mt) non-radiolabeled oligonucleotide probes in excess over labeled wildtype probes. Supershift was performed using an anti-HIF-1α antibody (Novus Biologicals).

FIG. 5. **The -1893 site binds *in vitro* generated HIF-1 complexes**. EMSA performed with [α-^{32}P]dATP-labeled probes, containing an *EPO* HBS (positive control) or the *ID2* promoter -1893-HBS, respectively. HIF-1 binding was assessed using HIF-1α (H) and ARNT (A) proteins, synthesized in rabbit reticulocyte lysate-based, coupled transcription/translation and subsequently associated for 30 min at room temperature before addition to binding reactions (H + A). As a negative control, pure reticulocyte lysate (L) was included. Supershift analysis was executed using antibodies directed against HIF-1α or ARNT (Novus Biologicals). Results are representative of several independent experiments with similar outcome.

FIG. 6. **HIF-1 binding is also detected at -725 within the *ID2* promoter**. EMSA demonstrating binding of HIF-1 complex proteins to the *ID2*-derived -725 HBS. Competition experiments were performed with indicated molar excess of unlabeled wildtype or mutated -

725-HBS oligonucleotides, respectively. Antibodies (1 l/lane) against HIF-1 and ARNT were used for verification of HIF-1 binding. Note that addition of HIF-1 or ARNT proteins alone were unable to induce shift of migration of the radiolabeled probes.

FIG. 7. **The -1893-HBS binds hypoxia-induced HIF-1**. EMSA using radiolabeled probes encompassing the *ID2*-derived HBS located at -1893 together with nuclear extracts (5 g/lane) from SK-N-BE(2) cells exposed to hypoxia, 1% O_2, (H) or normoxia (N) for 4 h. Competition analysis was executed with a molar excess of unlabeled oligonucleotide probes as indicated. For sequences of used probes, see Table 2.

FIG. 8. **HIF-1 binds the *ID2* promoter in DIP-treated SK-N-BE(2) neuroblastoma cells.** ChIP assay using SK-N-BE(2) cells treated with 200 M 2,2´-dipyridyl (DIP) or control (c) for 4 h. Cells were incubated with formaldehyde for crosslinking, and DNA was extracted and immunoprecipitated with anti-HIF-1 (HIF-1) or anti-human IgG (IgG) antibodies. After reversal of crosslinking, DNA was recovered and used in PCR for 35 cycles. *A*, Primers flanking respective *ID2* promoter HIF-binding site (HBS) were included in each reaction and generated 201 bp amplicons. *B*, As a positive control, PCR reactions containing immunoprecipitated DNA together with primers flanking the *VEGF* HBS, generating 135 bp amplicons, were performed. For input, DNA from non-immunoprecipitated extracts was used. A 50 bp DNA marker, M (Invitrogen), was run in parallel with indicated samples.

FIG. 9. **HIF-1 directs transcriptional activation of *ID2* from the functional HBSs**. HeLa cells (5 x 10^4) were transiently transfected by respectively 0.2 g/well of p*ID2*-1329wt plasmids, containing the -725 HBS, p*ID2*-2755 vector, containing the -1893 and -725 HBSs in wildtype (wt) or mutated (mt) form, empty pGL3-Basic vector or 0.2 g/well of the

positive control vector pHRE. Mutations of the respective HIF-binding sites are indicated as lower-case letters. Cotransfections were performed using 0.4 g/well of pFLAG-mHIF-1, expressing constitutively active HIF-1, or 0.4 g/well of empty pFLAG vector alone. Transfections were carried out overnight in OptiMEM I Reduced Serum Medium (Invitrogen) after which cells were again maintained in serum-containing medium. Cells were grown for an additional 24 hours and subsequently harvested in Passive Lysis Buffer (Promega). The luciferase reporter activity was then measured using the Dual-Luciferase Assay System according to the instructions supplied by the manufacturer (Promega). All transfections were performed in triplicates and data are representative of three independent experiments.

FIG. 10. **Molecular model for dedifferentiation in hypoxic neuroblastoma cells.** At normoxia, when ID proteins are expressed at moderate levels, neuronal marker genes are induced by the tissue specific bHLH proteins (i.e. HASH-1 and dHAND) in complex with E-proteins. During solid tumor growth, regions of intratumoral hypoxia emerge where hypoxia-inducible factors are stabilized. Within the bHLH network, the tissue specific transcription factors and obligate dimerization partners are downregulated through yet unknown mechanisms (19,20), in conjunction with a HIF-induced expression of ID2 (and potentially ID1), resulting in a downregulation of neuronal marker genes and a less differentiated phenotype.

Tables and Figures

TABLE 1**. Sequences of DNA primers used in the real-time quantitative PCR experiments.** All primer-pairs were designed by the Primer Express software (Applied Biosystems) and functionality was verified by standard measurements (data not shown).

Gene	Forward (5´ - 3´)	Reverse (5´ - 3´)
SDHA	TGGGAACAAGAGGGCATCTG	CCACCACTGCATCAAATTCATG
YWHAZ	ACTTTTGGTACATTGTGGCTTCAA	CCGCCAGGACAAACCAGTAT
HMBS	GGCAATGCGGCTGCAA	GGGTACCCACGCGAATCAC
UBC	ATTTGGGTCGCGGTTCTTG	TGCCTTGACATTCTCGATGGT
ID1	CTACGACATGAACGGCTGTTACTC	CTTGCTCACCTTGCGGTTCT
ID2	TCAGCCTGCATCACCAGAGA	CTGCAAGGACAGGATGCTGAT
ID3	TCAGCTTAGCCAGGTGGAAATC	TGGCTCGGCCAGGACTAC
VEGF	AGGAGGAGGGCAGAATCATCA	CTCGATTGGATGGCAGTAGCT

TABLE 2. ***ID2*-derived oligonucleotide probes used for electrophoretic mobility shift assays**. Only the sense DNA sequences are shown. For EMSAs, complementary probes were annealed with sense probes before binding reactions. The putative HIF-binding sites are shown in capitals and the mutations are underlined. Locations relative start of transcription are indicated for *ID2* and *EPO*, respectively.

Name	Sequence (5´-3´)	Location
-93-HBS	gataGACGTGccaccttc	-97/ -80
-105-HBS	cccgCTCGTCttgataga	-109/ -92
-301-HBS	atccCTCGTCccgcatcc	-305/ -288
-725-HBS	cgaaTGCGTGcgtgggtggtt	-729/ -713
-734-HBS	gcctGTCGTCgaatgcgt	-738/ -725
-1588-HBS	ctgtCACGTGacggtcag	-1592/ -1575
-1611-HBS	gagaGGCGTCatggggcg	-1615/ -1598
-1893-HBS	gtggCACGTAtgtgacag	-1897/ -1880
mt-725-HBS	cgaaTG<u>AA</u>TGcgtgggtggtt	-729/ -713
mt-1893-HBS	gtggCA<u>AT</u>TAtgtgacag	-1897/ -1880
wt-EPO-HBS	gcccTACGTGctgtctca	+3065/ +3082 (From (9))
mt-EPO-HBS	gcccTA<u>TAGA</u>ctgtctca	+3065/ +3082 (From (9))

FIG. 1

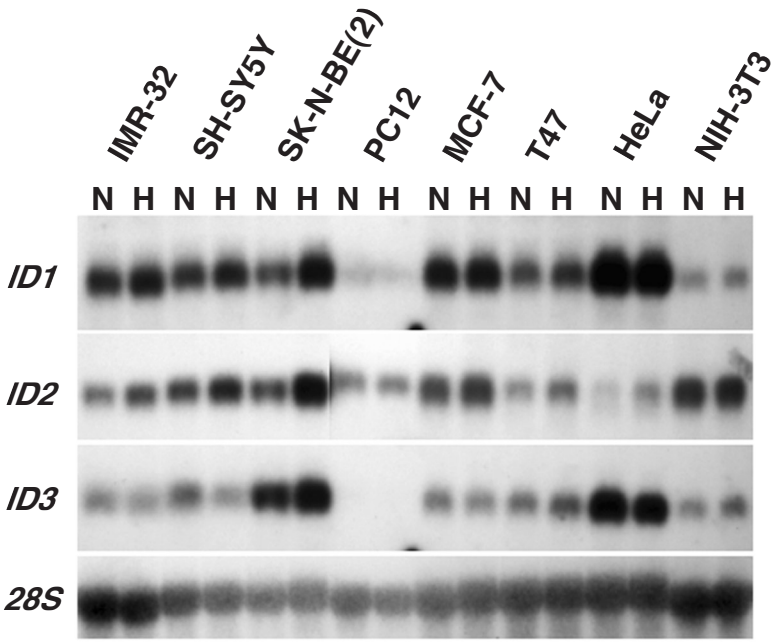
IMR-32
SH-SY5Y
SK-N-BE(2)
PC12
MCF-7
T47
HeLa
NIH-3T3
N H N H N H N H N H N H N H N H
ID1
ID2
ID3
28S

FIG. 2

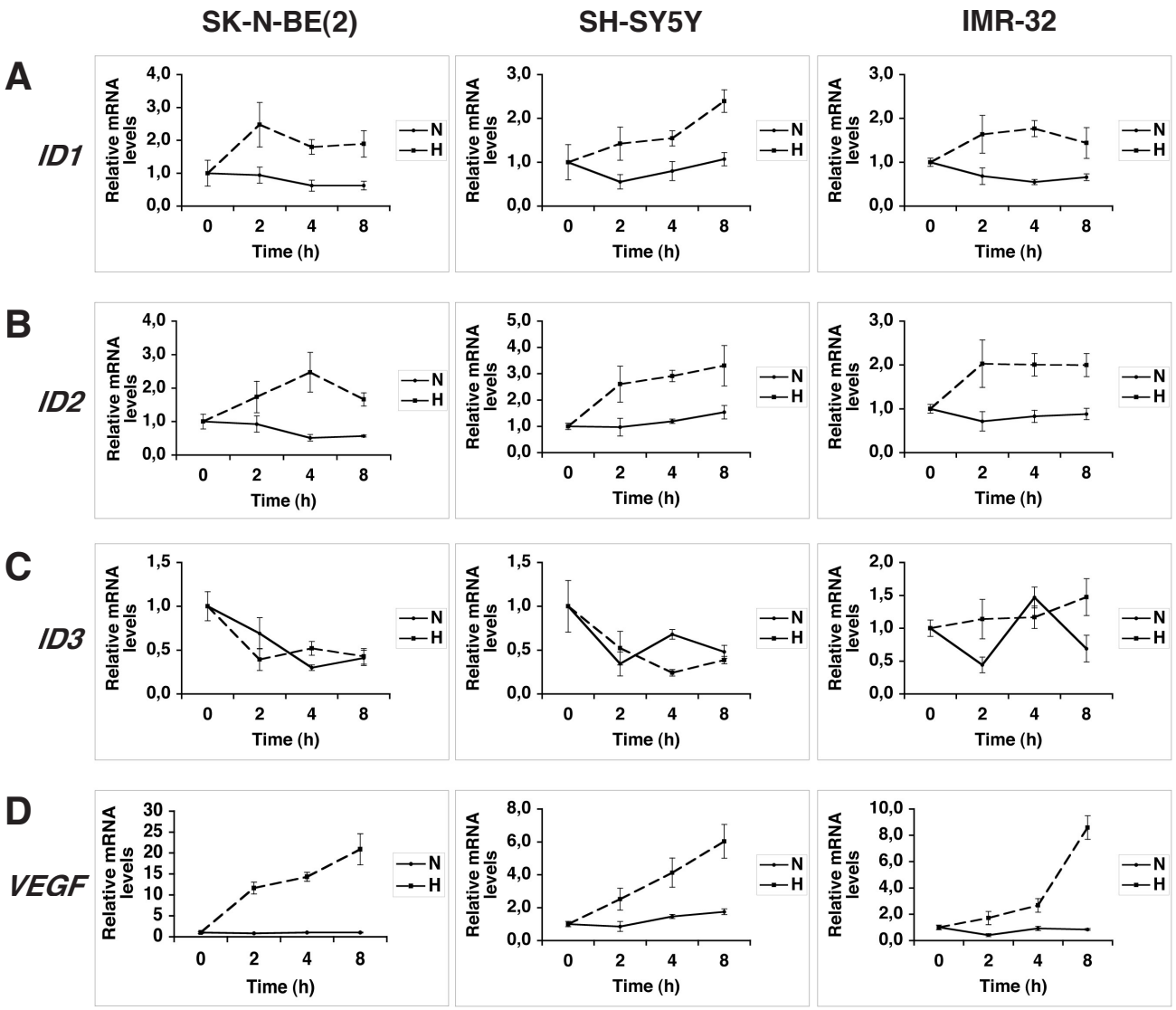
SK-N-BE(2)
SH-SY5Y
IMR-32
A
ID1
B
ID2
C
ID3
D
VEGF
Relative mRNA levels
Time (h)
N
H

FIG. 3

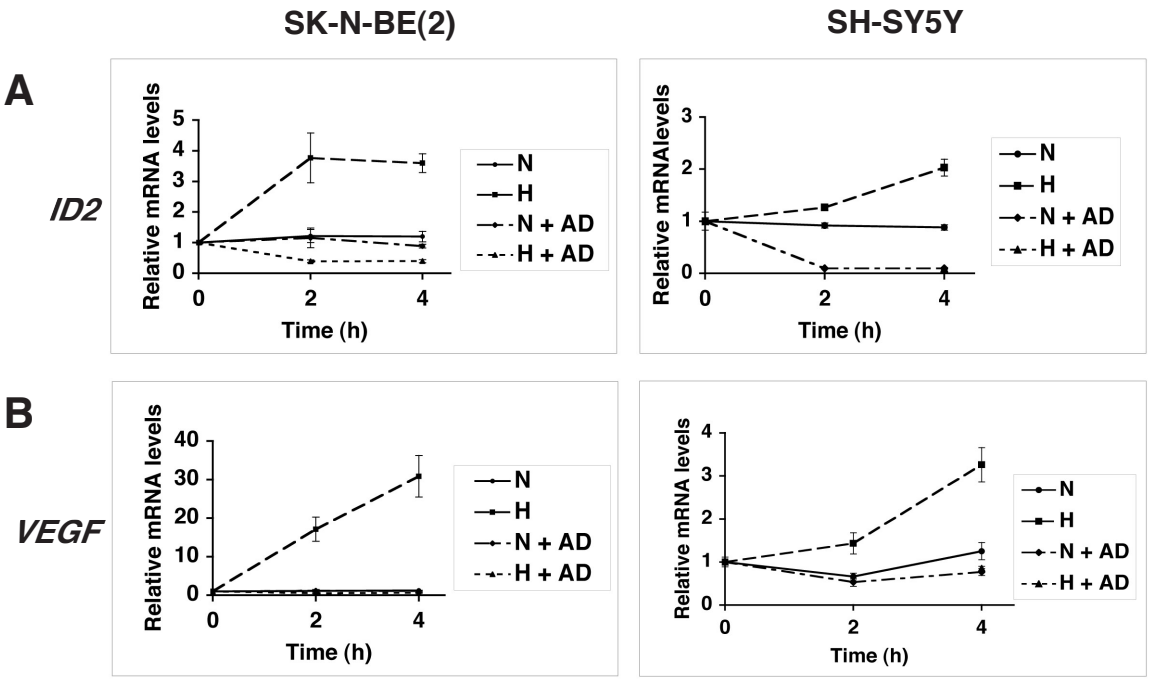
SK-N-BE(2)
SH-SY5Y
A
ID2
B
VEGF
Relative mRNA levels
Time (h)
N
H
N + AD
H + AD

FIG. 4

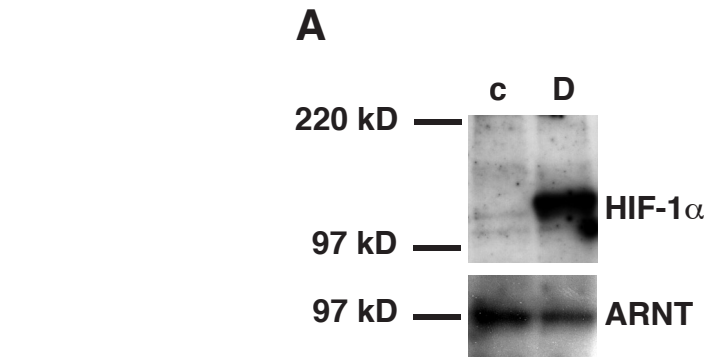
A
c
D
220 kD
97 kD
HIF-1α
97 kD
ARNT

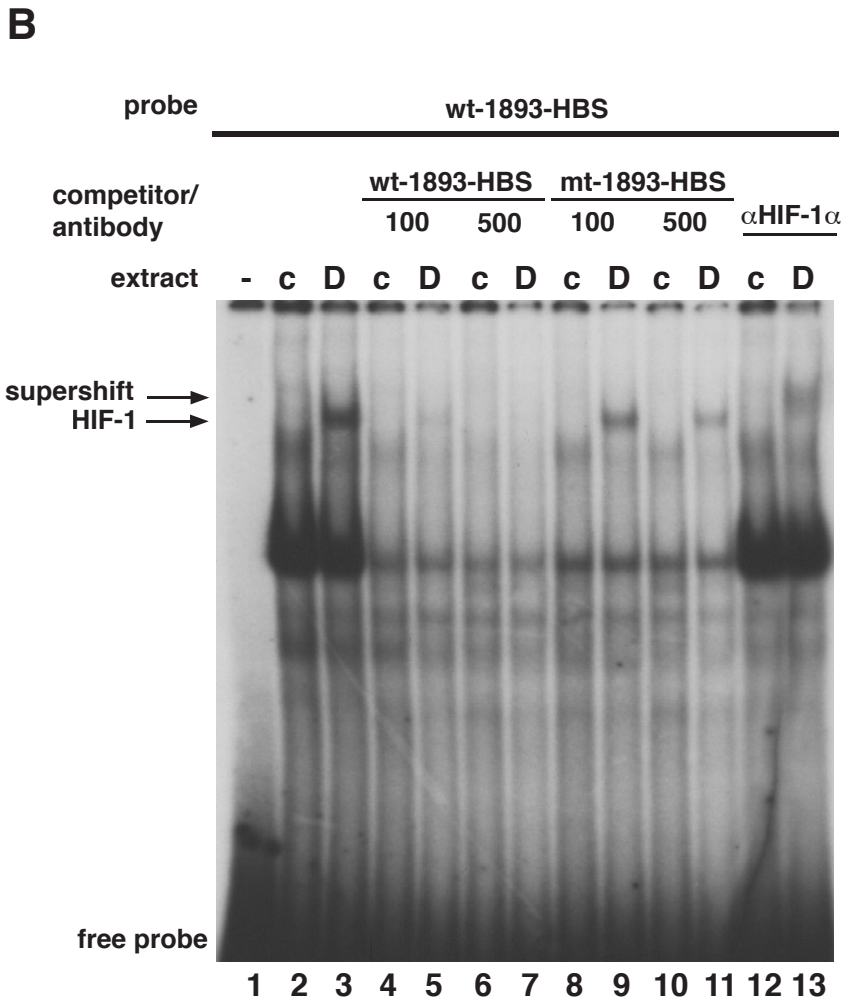
B
probe
wt-1893-HBS
competitor/
antibody
wt-1893-HBS
mt-1893-HBS
100
500
100
500
αHIF-1α
extract
- c D c D c D c D c D c D
supershift
HIF-1
free probe
1 2 3 4 5 6 7 8 9 10 11 12 13

FIG. 5

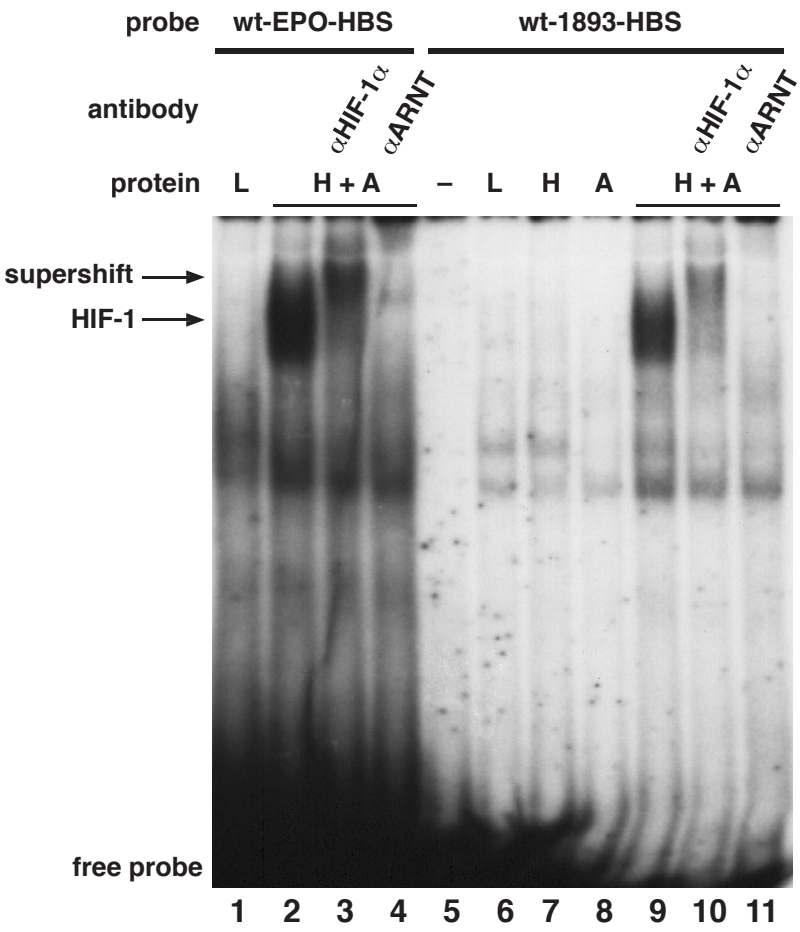
probe
wt-EPO-HBS
wt-1893-HBS
antibody
αHIF-1α
αARNT
αHIF-1α
αARNT
protein
L
H + A
–
L
H
A
H + A
supershift
HIF-1
free probe
1 2 3 4 5 6 7 8 9 10 11

FIG. 6

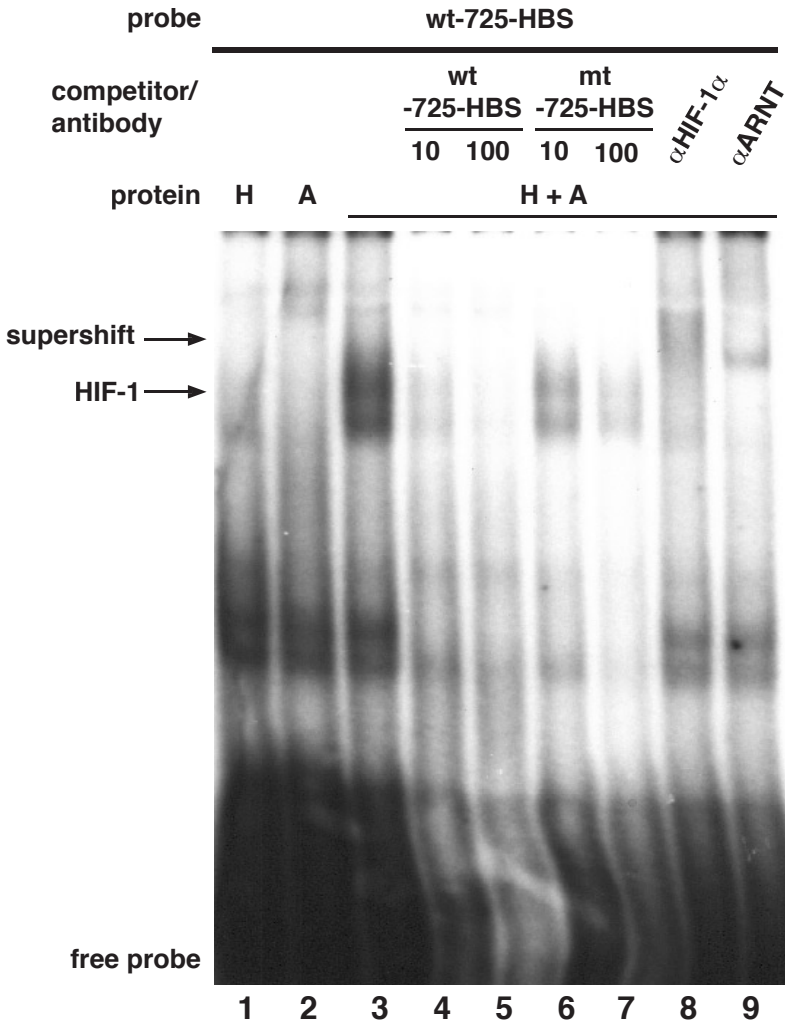
probe
wt-725-HBS
competitor/
antibody
wt
-725-HBS
mt
-725-HBS
10
100
10
100
αHIF-1α
αARNT
protein
H
A
H + A
supershift
HIF-1
free probe
1
2
3
4
5
6
7
8
9

FIG. 7

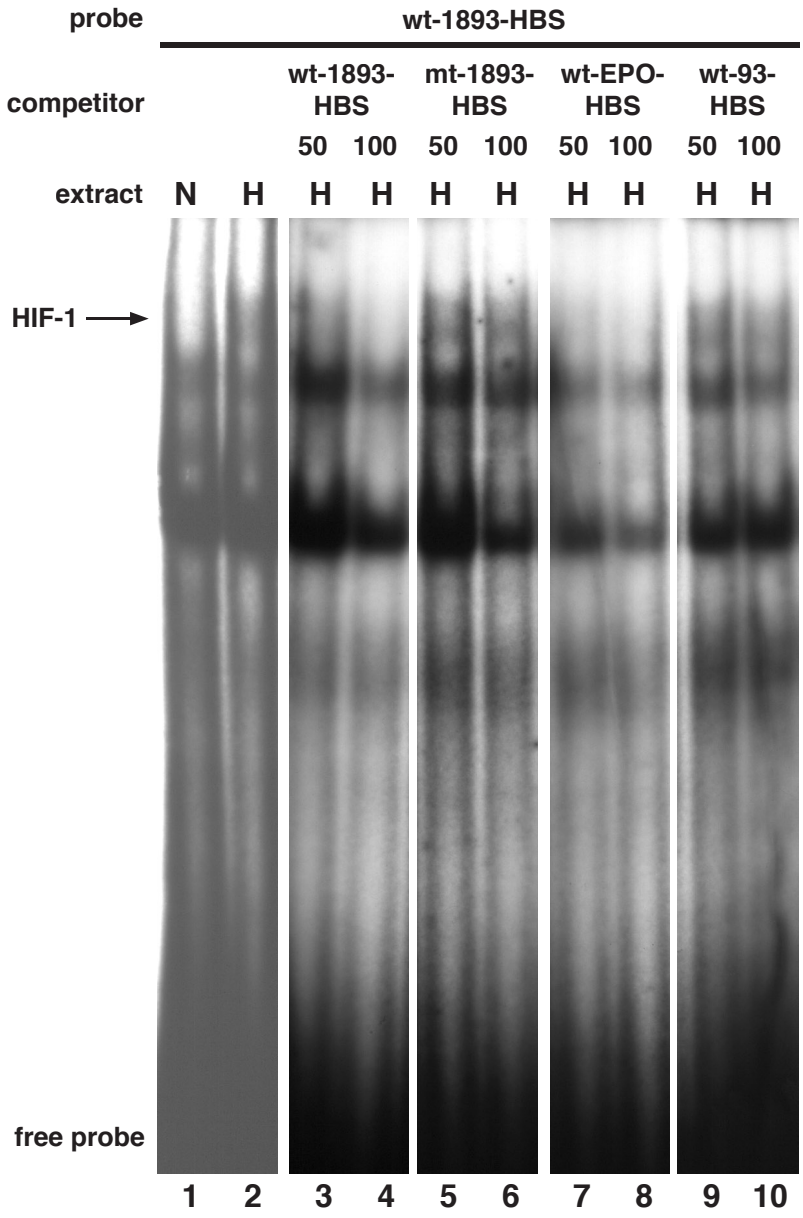
probe
wt-1893-HBS
competitor
wt-1893-HBS
mt-1893-HBS
wt-EPO-HBS
wt-93-HBS
50 100 50 100 50 100 50 100
extract
N H H H H H H H H H
HIF-1
free probe
1 2 3 4 5 6 7 8 9 10

FIG. 8

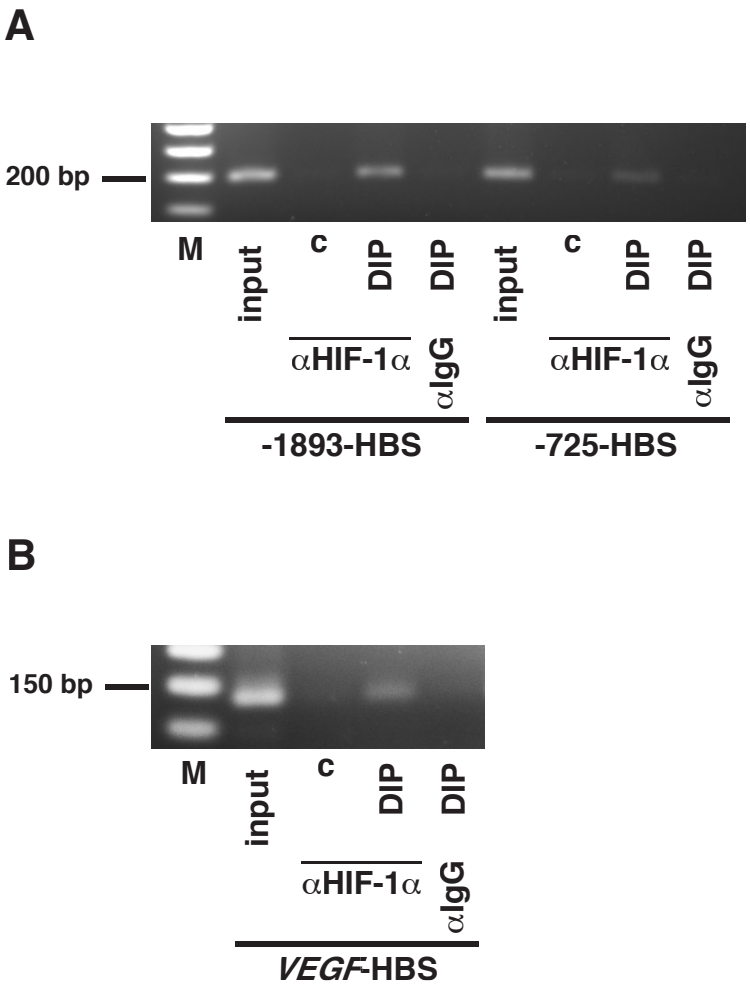
A
200 bp
M
input
c
DIP
DIP
input
c
DIP
DIP
αHIF-1α
αIgG
αHIF-1α
αIgG
-1893-HBS
-725-HBS
B
150 bp
M
input
c
DIP
DIP
αHIF-1α
αIgG
VEGF-HBS

FIG. 9

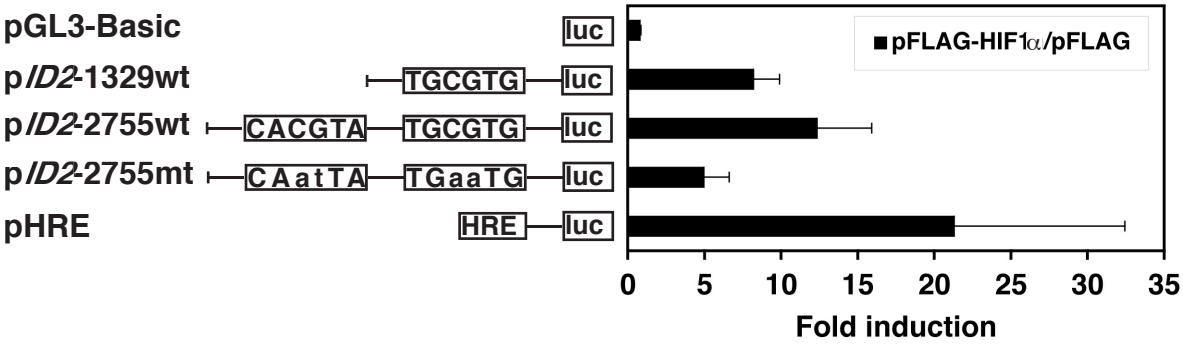
pGL3-Basic
luc
p*ID2*-1329wt
TGCGTG
luc
p*ID2*-2755wt
CACGTA
TGCGTG
luc
p*ID2*-2755mt
CAatTA
TGaaTG
luc
pHRE
HRE
luc
pFLAG-HIF1α/pFLAG
0
5
10
15
20
25
30
35
Fold induction

FIG. 10

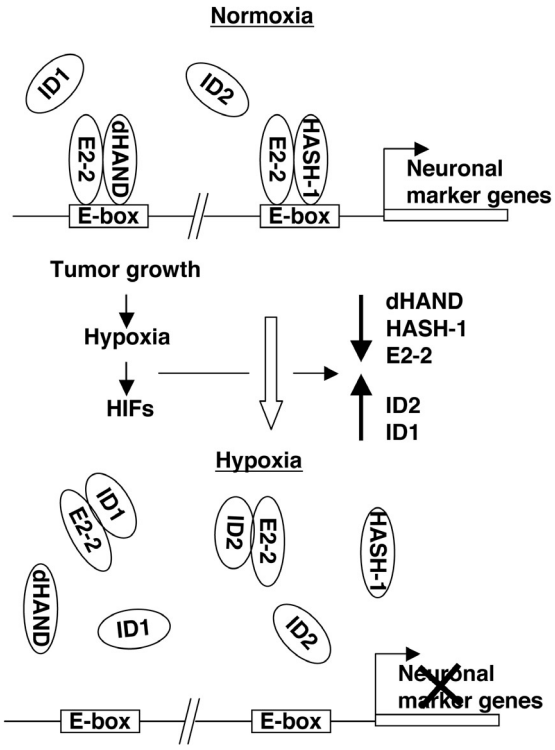
Normoxia
ID1
ID2
E2-2
dHAND
E2-2
HASH-1
Neuronal
marker genes
E-box
E-box
Tumor growth
Hypoxia
HIFs
dHAND
HASH-1
E2-2
ID2
ID1
Hypoxia
ID1
E2-2
ID2
E2-2
HASH-1
dHAND
ID1
ID2
Neuronal
marker genes
E-box
E-box